

0
ADA 121879

MODELING THE INFRARED
EMITTANCE OF PAINTS

FINAL REPORT
to
U. S. Army Mobility Equipment
Research and Development Command

by
James R. Aronson and Alfred G. Emslie
ARTHUR D. LITTLE, INC.
Cambridge, Massachusetts 02140

DTIC
ELECTED
NOV 29 1982
S D

Contract No. DAAK70-79-D-0036
Task Order No. 0008
ADL Reference No. 83670-28

October 1980

DISTRIBUTION STATEMENT A

Approved for public release
Distribution Unlimited

82 11 29 102

Arthur D Little Inc

FILE COPY

UNCLASSIFIED

SECURITY CLASSIFICATION OF THIS PAGE (When Data Entered)

REPORT DOCUMENTATION PAGE		READ INSTRUCTIONS BEFORE COMPLETING FORM
1. REPORT NUMBER	2. GOVT ACCESSION NO.	3. RECIPIENT'S CATALOG NUMBER
	AD-A121879	
4. TITLE (and Subtitle) MODELING THE INFRARED EMITTANCE OF PAINTS		5. TYPE OF REPORT & PERIOD COVERED Final - March 1980 - September 1980
		6. PERFORMING ORG. REPORT NUMBER ADL-83670-28
7. AUTHOR(s) James R. Aronson and Alfred G. Emslie		8. CONTRACT OR GRANT NUMBER(s) DAAK70-79-D-0036 Task Order 0008
9. PERFORMING ORGANIZATION NAME AND ADDRESS Arthur D. Little, Inc. Acorn Park Cambridge, Massachusetts 02140		10. PROGRAM ELEMENT, PROJECT, TASK AREA & WORK UNIT NUMBERS
11. CONTROLLING OFFICE NAME AND ADDRESS U.S. Army Mobility Equipment Research and Development Command (MERADCOM) Fort Belvoir, Virginia 22060		12. REPORT DATE October 1980
14. MONITORING AGENCY NAME & ADDRESS (if different from Controlling Office)		13. NUMBER OF PAGES 46
		15. SECURITY CLASS. (of this report) UNCLASSIFIED
		15a. DECLASSIFICATION/DOWNGRADING SCHEDULE N/A
16. DISTRIBUTION STATEMENT (of this Report) Distribution Unlimited		
17. DISTRIBUTION STATEMENT (of the abstract entered in Block 20, if different from Report)		
18. SUPPLEMENTARY NOTES		
19. KEY WORDS (Continue on reverse side if necessary and identify by block number) Infrared Emittance of Paints Reflectance of Paints Camouflage		
20. ABSTRACT (Continue on reverse side if necessary and identify by block number) Present day camouflage paints are ineffective in the thermal infrared spectral region. In order to develop improved paints or coatings, a theoretical understanding of the factors involved is required. To this end modification of a previously developed theory of the emittance of particulate systems has been undertaken. Infrared spectral measurements of the Army's Forest Green Paint have been made and compared with computer simulations based on the modified theory. The results suggest where changes in present formulations need to be made to develop improved paints. (over)		

20. The most important change is the substitution of an infrared transparent binder for the opaque one currently used. If this binder can be developed from a material with visible refractive index near 1.5, the visible properties of the paint will be minimally affected.

Accession For	
NTIS GRA&I	<input checked="" type="checkbox"/>
DTIC TAB	<input type="checkbox"/>
Unannounced	<input type="checkbox"/>
Justification	
By _____	
Distribution/ _____	
Availability Codes	
Dist	Avail and/or Special
A	



UNCLASSIFIED

TABLE OF CONTENTS

<u>Section</u>	<u>Page</u>
I Introduction	1
II Theory	5
III Experimental Measurements	7
IV Optical Constants (Complex Refractive Indices)	29
V Comparison of Theoretical Simulations with Experimental Measurements	36
VI Suggestions for Further Work	41
VII References	42
Appendix 1	43
Theory of the Spectral Reflectance of a Layer of Paint on a Substrate	

LIST OF FIGURES

<u>Figure No.</u>		<u>Page</u>
1	Pellet Spectrum of AIG	9
2	Fit to Reflectance of AIG	10
3	Pellet Spectrum of Chrome Yellow	11
4	Fit to Reflectance of Crocoite	12
5	Pellet Spectrum of Diatomaceous Earth in KBr	13
6	Pellet Spectrum of Talc in KBr	14
7	Pellet Spectrum of Carbazole Dioxazine Violet in KBr	15
8	Alkyd Resin Film Transmittance at Brewster Angle	16
9	Pellet Spectrum of Molybdate Orange	17
10	Emittance Spectra of Forest Green Systems	19
11	Auxiliary Emittance Data	21
12	Reflectance of Forest Green Paint	22
13	Reflectance of Forest Green 4	23
14	Reflectance of Forest Green 6 vs Diffuse Reference	24
15	Comparison of Emittance and Reflectance Data for Forest Green 6	25
16	Reflectance of Alkyd and Polyurethane Binders on Aluminum	27
17	Fit to Alkyd Resin Transmittance	32
18	Pigment Particle Size Distribution	37
19	Comparison of Theoretical Simulations of Forest Green 6 Paint with Experimental Data	38
20	Comparison of Coarse, Fine, and Bridged Theory Simulations with Experimental Data	39

I. Introduction

Camouflage paints designed to aid in the concealment of military objects in the visible and near infrared spectral regions would only fortuitously accomplish this task in other regions of the spectrum as well. However, it has recently become a major concern of various parts of the United States Department of Defense and specifically the MERADCOM camouflage laboratory to be able to develop paints or coatings that would simultaneously be effective in the thermal infrared region of the spectrum, and the shorter wave near infrared portion of the spectrum while not degrading their performance in the visible region. The vital importance of the thermal infrared region which we will define here as principally the 8-14 μm region but including the 3-5 μm region as well, has become of continually greater concern owing to the rapid development of thermal imaging systems notably FLIRs, and other line scanners in which the platform provides the extra dimension for construction of the image. The extreme sensitivity of these devices and their present availability even in the commercial world has dictated that scientists, engineers, and paint technologists concerned with these problems devote a considerable amount of effort to improving the camouflage in the thermal infrared region.

This problem is technologically related to one that Arthur D. Little scientists have worked on over the last decade - that of infrared remote sensing of the composition of a planetary surface. In our previous work on the problem of planetary surface remote compositional sensing, we discovered that while suitable data in the infrared region could readily be obtained, there was no comprehensive theoretical method available to predict, model or fully understand the ways in which the signature of a mixture of materials would vary with the amounts,

particle sizes, and components of the mixture. To fill this need, we constructed a theoretical model of reflectance or emittance of a mixture of minerals¹ and carried out a number of experimental measurements on powders to aid in construction of the model^{2,3}. The only existing exact theory related to such problems is the Mie theory⁴ but it in fact only describes the absorbing and scattering behavior of isolated spherical particles. Problems rendering this theory incorrect for mixtures of mineral particles and indeed for paints are related both to the Mie theory requirements for sphericity and for isolation of the individual particles. The theory that we developed treats the individual particles as being randomly oriented, jagged in nature, and uses a modified six beam theory of radiative transfer related to the Kubelka-Munk⁵ formulation. The entire theory is described in a number of publications^{1,2,3} but for the purposes of this report it is sufficient to note that computer calculations based on this theory successfully simulate to a high degree the spectral signatures of various minerals and mixtures of minerals including lunar soils⁶ such that we can now successfully model the expected spectrum from mixtures of materials of varying volume fractions and particle sizes or particle size distributions.

The theory is made up of two subtheories, one for particles large compared to the radiation wavelength, and one for particles small compared to the radiation wavelength. The coarse particle theory is based on geometrical optics for spheres but modified by the wave optical effects of edges and other asperities on the surface of the spheres and by the proximity of neighboring particles. The fine particle theory is based on the Lorentz-Lorenz theory of dielectrics and treats particles small compared to the radiation wavelength by recognizing that the radiation necessarily samples "averaged" optical properties using the Lorentz-Lorenz theory to calculate

the average. The two theories are merged by an empirical bridging relationship which has been found to provide better agreement with experimental results in the intermediate region than either theory alone.

The successful comparisons of simulations and experimental results³ show that in great detail the physical mechanisms of scattering and absorption by particulate media are well understood and represented by this theory. This understanding led us to believe that a similar theory could be constructed for fibrous materials. The modified theory proved to be quite able to predict the spectral reflectance or emittance of fibrous materials as a function of fiber diameter, filling factors and the packing in individual fiber bundles⁷.

These two successful uses of the general theory led us to believe that the modeling of a paint or coating would also succeed. We therefore began to carry out the necessary modifications of the theory for work in the near infrared region of the spectrum under a previous contract. At MERADCOM's request, we enlarged the scope of this previous work to include the thermal infrared region of the spectrum owing to the vital nature of this region in present day military considerations. It was decided that we should establish the accuracy of the theory and refine it where necessary by modeling one of the Army's existing paint formulations; the one chosen is Forest Green. However, early in this work some obvious practical considerations became apparent with regard to the nature of the problem of designing improved paints or coatings for this region. These will be discussed later in the body of the report.

In Section II, we will discuss the theoretical changes required to convert the pre-existing model of the reflectance or emittance of particulate surfaces to the case of particles in a binder as in camouflage paint. In Section III, we will discuss the experimental part of our program - the Forest Green

paint formulation and the subformulations that we obtained in order to carry out some modeling prior to obtaining all the required input parameters for all of the components of Forest Green paint. In Section IV, we present the optical constant methodology and results during our first six months effort. Finally, in Section V, we will show the fit between theory and experiment and in Section VI, present suggestions for further work.

II Theory

We began with the theory as presented in references 1, 2, and 3. The most fundamental theoretical changes required were to provide for the occurrence of surface reflectance terms originating in the external reflection of the incident beam by the Fresnel relations. It has always been part of our methodology to calculate reflectance rather than emittance as it is intuitively more obvious to most readers as well as to the authors. However, the emittance can be obtained from the reflectance by the use of Kirchhoff's law for opaque substances. That law which is that absorptance equals emittance leads to the formula;

$$\epsilon = 1 - R$$

Where ϵ is the emittance of the material and R is its reflectance. Both quantities may be subscripted with the angular specifications. That is, the Kirchhoff complement of the reflectance at some angle must be the emittance at that same angle. As reflectance requires two subscripts and emittance only one, analysis shows⁸ that emittance may be treated as if the incident beam was coming from inside the medium and entirely diffuse. That is, the proper complement of the emittance at 30° is the reflectance in which the surface is illuminated diffusely (hemispherically) and reflectance is measured at 30° or conversely the surface is illuminated at 30° and the reflectance is measured diffusely.

The surface term R_e in our present formulation refers to the value obtained by integrating the Fresnel relations over all angles, i.e., diffuse reflectance. Associated with this diffuse term for external Fresnel reflectance is an internal term R_i which is equal to

$$R_i = 1 - \frac{(1-R_e)}{n^2}$$

In addition to these surface terms, we also had to derive a formula including the volume reflectance resulting from a finite paint layer on a substrate of reflectance R_g . This formula is:

$$R = \frac{[R_e(1-R_i R_v)(1-R_v R_g) - R_e(R_v - R_i)(R_v - R_g) e^{-2\gamma x} + (1-R_e)(1-R_i)R_v(1-R_v R_g) - (1-R_e)(1-R_i)(R_v - R_g) e^{-2\gamma x}]}{[(1-R_i R_v)(1-R_v R_g) - (R_v - R_i)(R_v - R_g) e^{-2\gamma x}]}$$

where x is the thickness of the paint layer, R_v is the volume diffuse reflectance for an infinitely thick layer and $\gamma = (K^2 + 2KS)^{1/2}$. K and S are the usual absorption and back-scattering coefficients given in our previous work¹. The derivation of this formula is given in Appendix 1.

Strictly speaking, R_g refers to the reflectance of the underlying substrate as modified by the overcoating layer. However, as the reflectance of metal surfaces are not greatly affected by this consideration, we have used the directly observed reflectance $(1-\epsilon)$ of our substrate aluminum plate in our calculations thus far. The R_e and R_i for the fine particle theory are calculated from the Lorentz-Lorenz¹ complex index of refraction but in the coarse particle theory we have made the assumption that the only coherent surface terms arise from the matrix so that these terms are calculated for the matrix material as if it were totally covering the surfaces of the pigment particles. All pigment contributions are included in the volume term. Finally, as our previous theories always assumed particle-vacuum or particle-air interfaces only, the change was made to particle-matrix interfaces by dividing particle complex indices of refraction by the real part of the matrix complex index of refraction. Wavelength dependent effects were likewise adjusted to the index in the medium where necessary.

III. Experimental Measurements

As previously mentioned, we have chosen to carry out our modeling experiments using the Army's Forest Green paint at the suggestion of Dr. Jay Fox then of MERADCOM. This is a complex material composed of an alkyd binder - four pigments and two extender pigments. The composition is shown in Table 1.

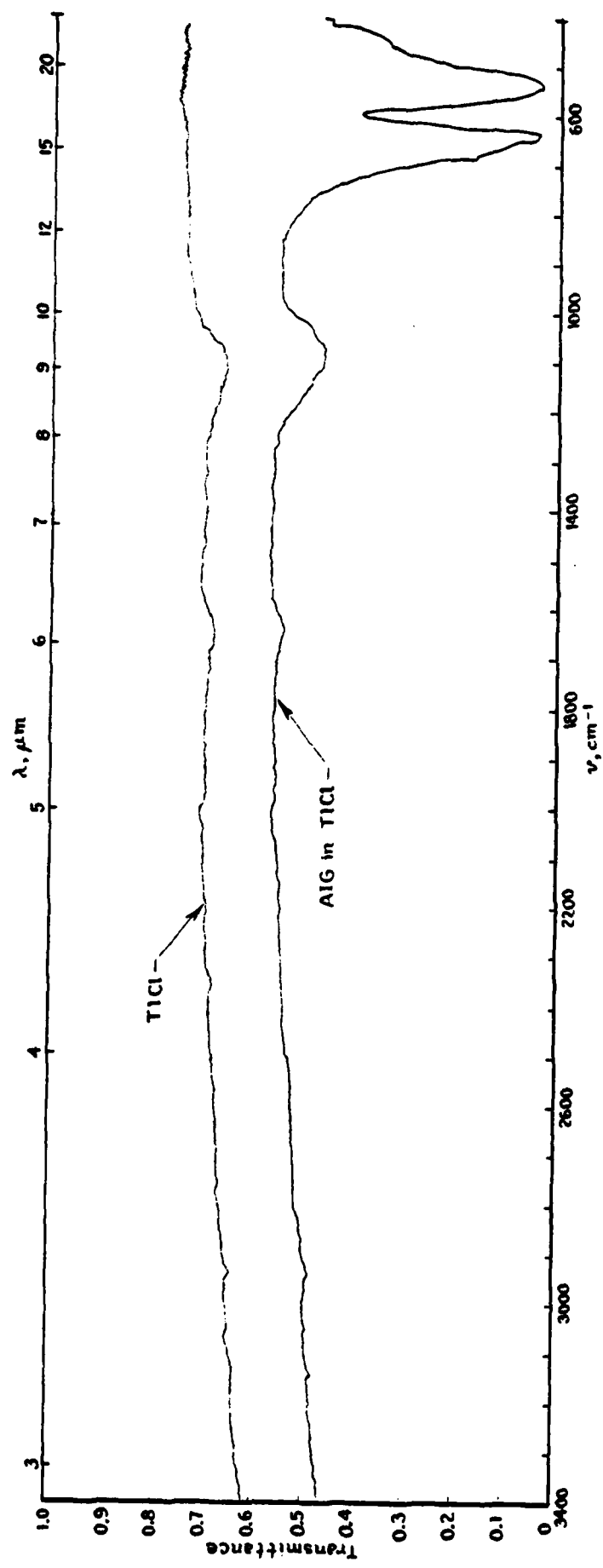
Table I

Compositions of Forest Green Formulations

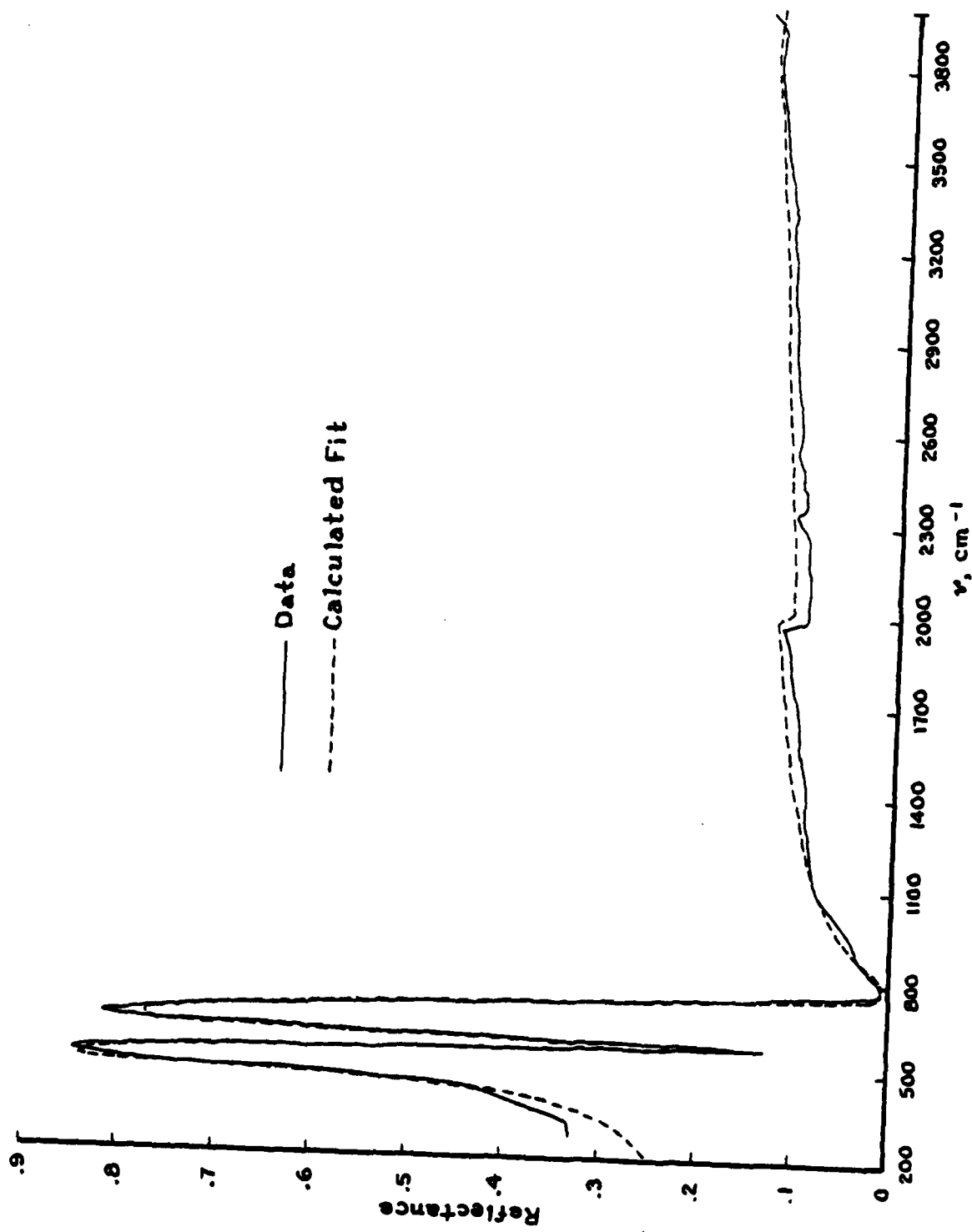
<u>Component</u>	<u>Volume Fractions in Dry Paint</u>				
	<u>Forest Green</u>	<u>(Sub Formulations)</u>			
	<u>MIL-E52798</u>	<u>FG2</u>	<u>FG3</u>	<u>FG4</u>	<u>FG6</u>
1) Acid Insoluble Green Pigment (Ferro V-11655) (Co,Cr,Zn,Ti Spinel)	0.101	0.103	0.106	0.117	0.133
2) Chrome Yellow (med) (PbCrO ₄)	0.026	0.027	-	-	-
3) Molybdate Orange	0.008	-	-	-	-
4) Cyandur Violet (Carbazole Dioxazine Violet)	0.010	-	-	-	-
5) Talc (Nytal 300)	0.093	0.093	0.097	-	-
6) Diatomaceous Earth (Celite 110)	0.175	0.175	0.183	0.203	-
7) Alkyd Resin (Solids Only) (Beckosol 11-070)	0.587	0.602	0.614	0.680	0.867

Previous work under joint sponsorship of MERADCOM, NARADCOM and the Army Research Office indicated that the near infrared spectrum of this material is dominated by the acid insoluble green pigment, as is true to a lesser extent in the visible region. In the visible region for which this material was originally designed, the various ingredients performed their functions to suitably blend with the chlorophyll spectrum. If it were only for the near infrared region, none of the other tinting pigments would be required and only the extender pigments whose purpose it is to make the paint into the matte finish i.e., scatter diffusely would be required. We will digress at this point to observe that the WARSAW pact nations allow their paints to have some gloss in contrast to the way our paints are designed. The acid insoluble green pigment (AIG) is a mixed oxide of zinc, chromium, titanium, and cobalt having a spinel structure. The transmission spectrum of powdered AIG dispersed in a pellet made of thallium chloride is shown in Figure 1, while a reflection spectrum obtained from a sample which was hot pressed to high density and polished is shown in Figure 2. A pellet spectrum of lead chromate is shown in Figure 3 and the reflection spectrum of a single crystal of this compound, the relatively rare mineral known as crocoite, obtained from the Harvard University collection is shown in Figure 4. Pellet spectra of the diatomaceous earth, the talc, and the carbazole dioxazine violet are shown in Figures 5, 6 and 7, while the transmission spectrum of a thin film of the alkyd resin is shown in Figure 8. A spectrum of molybdate orange from the literature⁹ is shown in Figure 9.

In order to obtain the optical constants (complex index of refraction) of these various components of the Forest Green paint, quantitative data had to be obtained and reduced. Our method of reduction from reflectance spectra is given in reference 10. None of the pellet spectra are suitable for such a purpose except with large relative error. Inasmuch as a quantitative treatment of transmission through a pellet is very

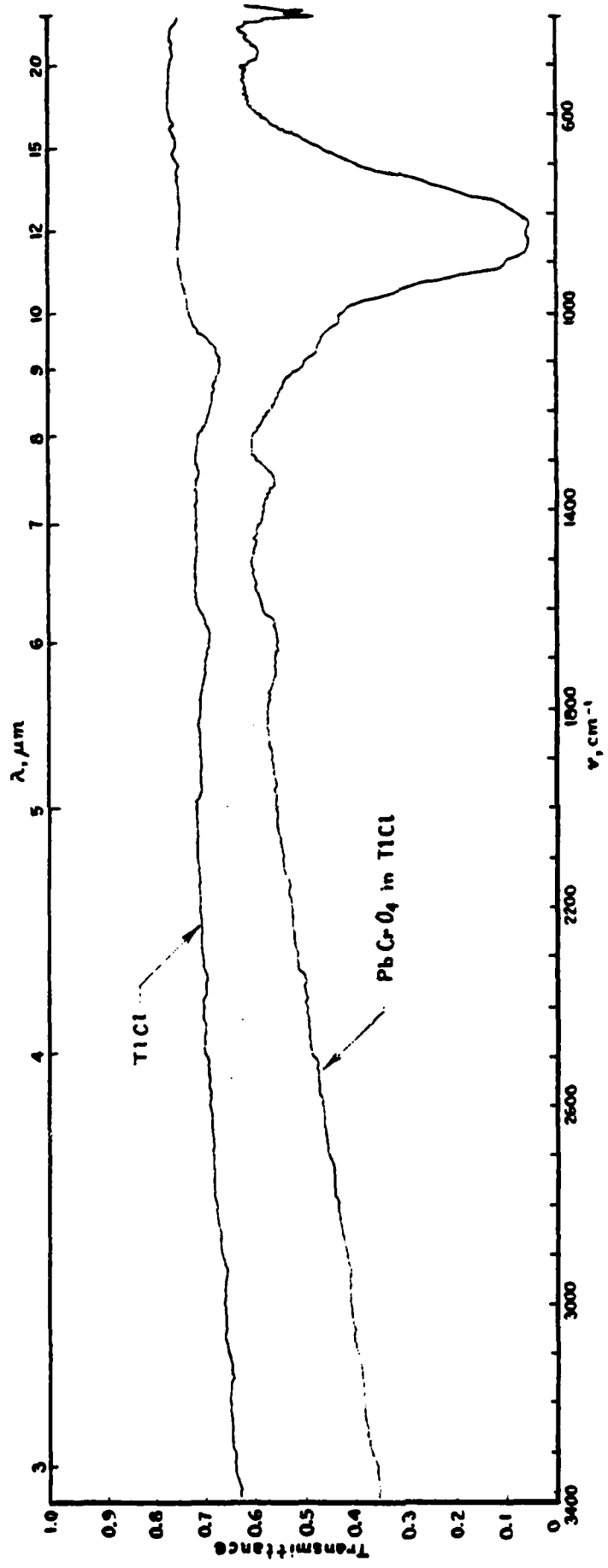


PELLET SPECTRUM OF AlG
Figure 1



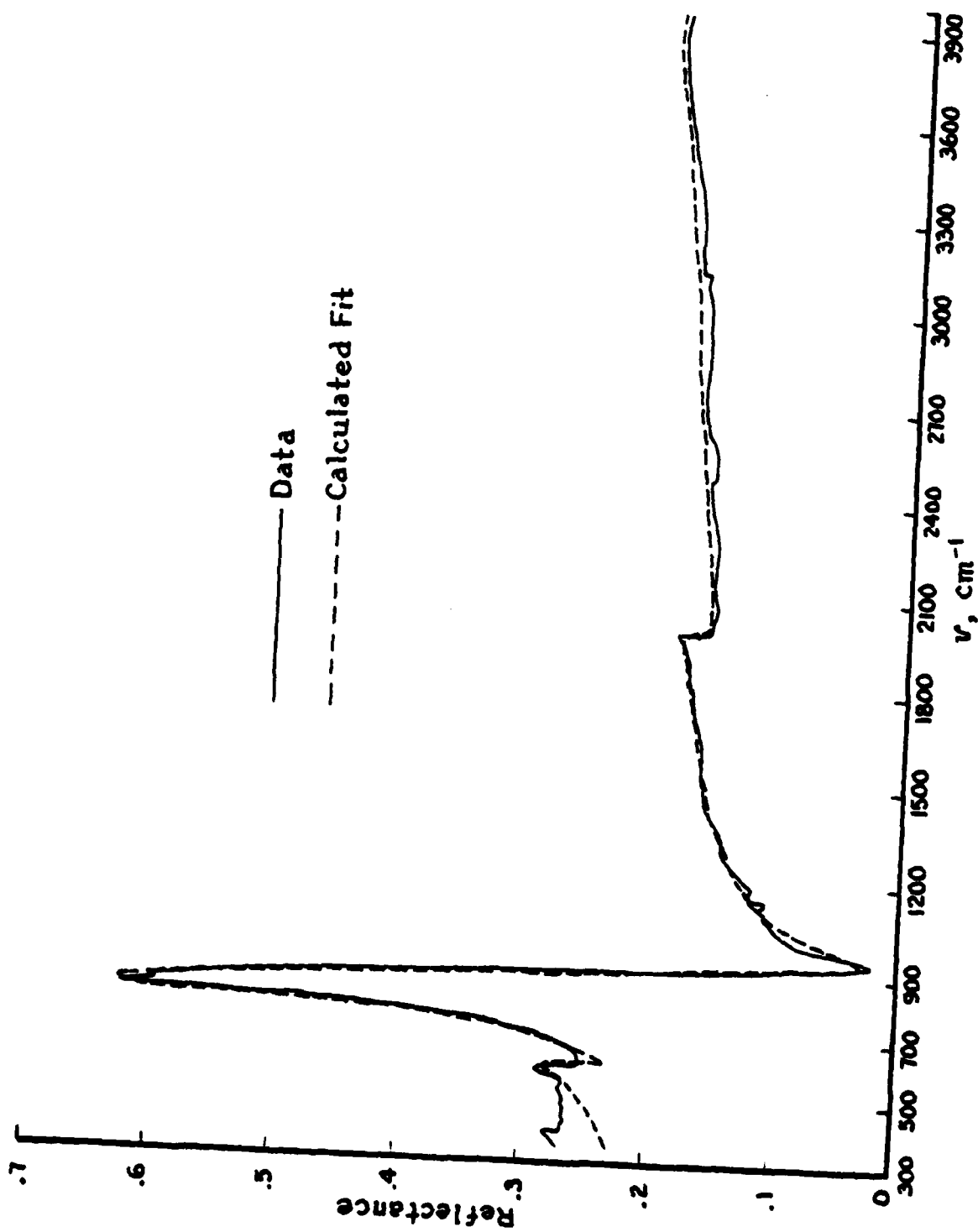
FIT TO REFLECTANCE OF AIG

Figure 2



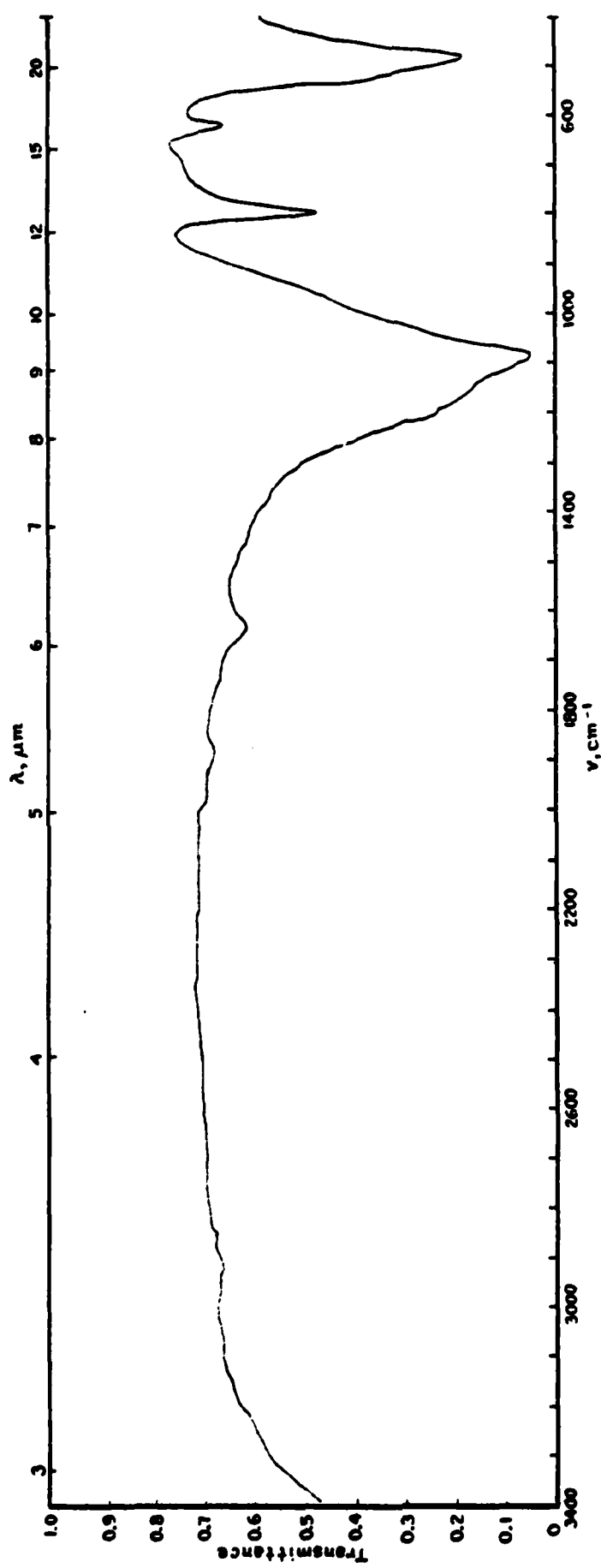
PELLET SPECTRUM OF CHROME YELLOW

Figure 3



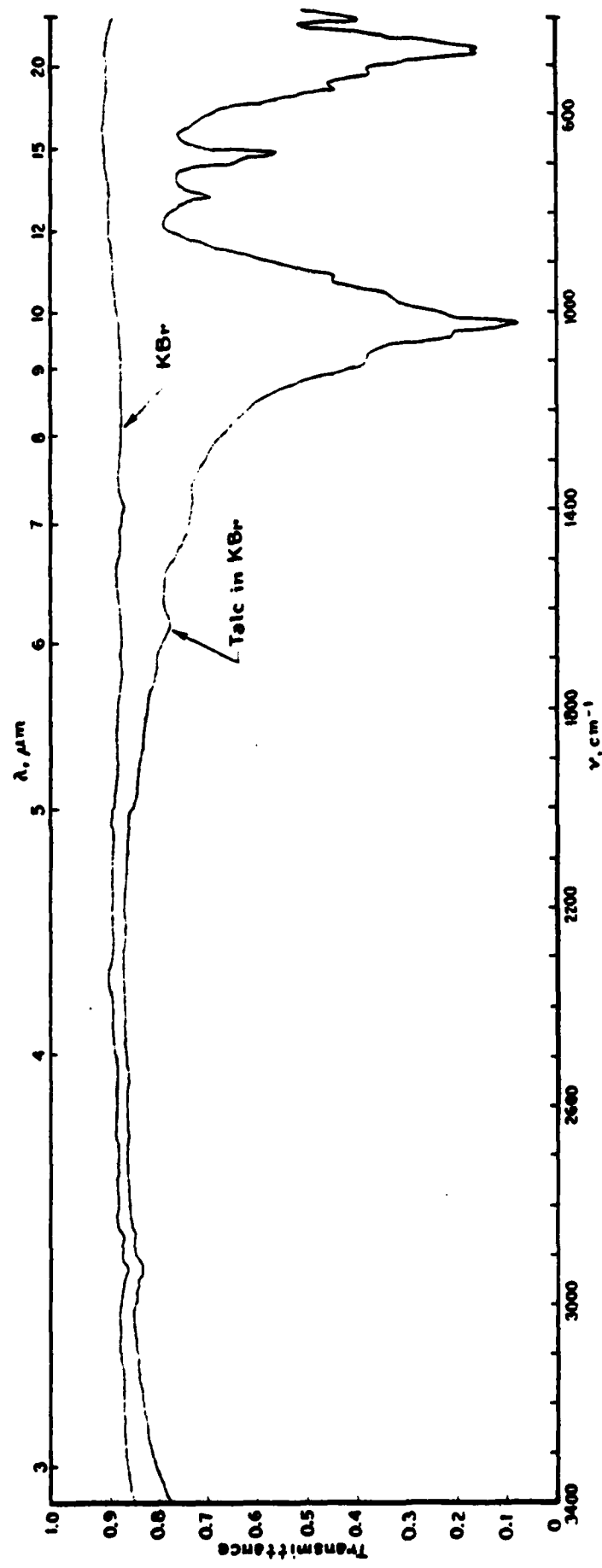
FIT TO REFLECTANCE OF CROCOITE

Figure 4



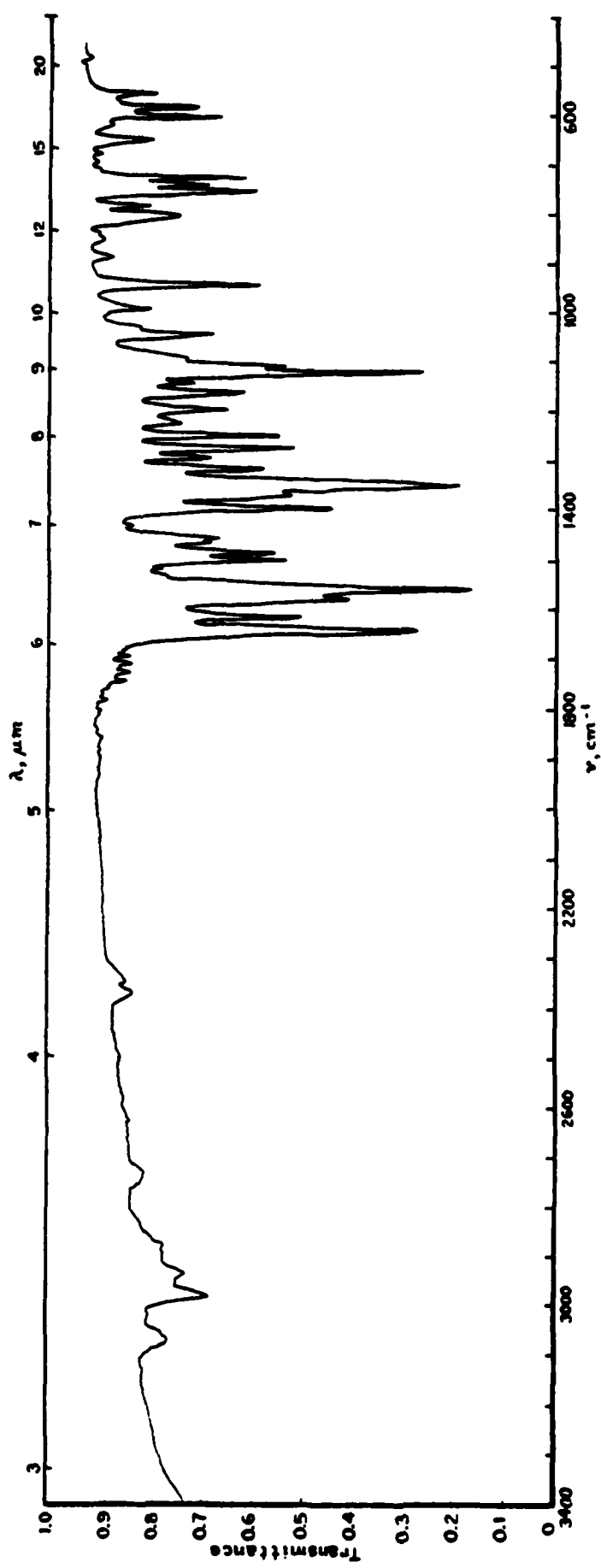
PELLET SPECTRUM OF DIATOMACEOUS EARTH IN KBr

Figure 5



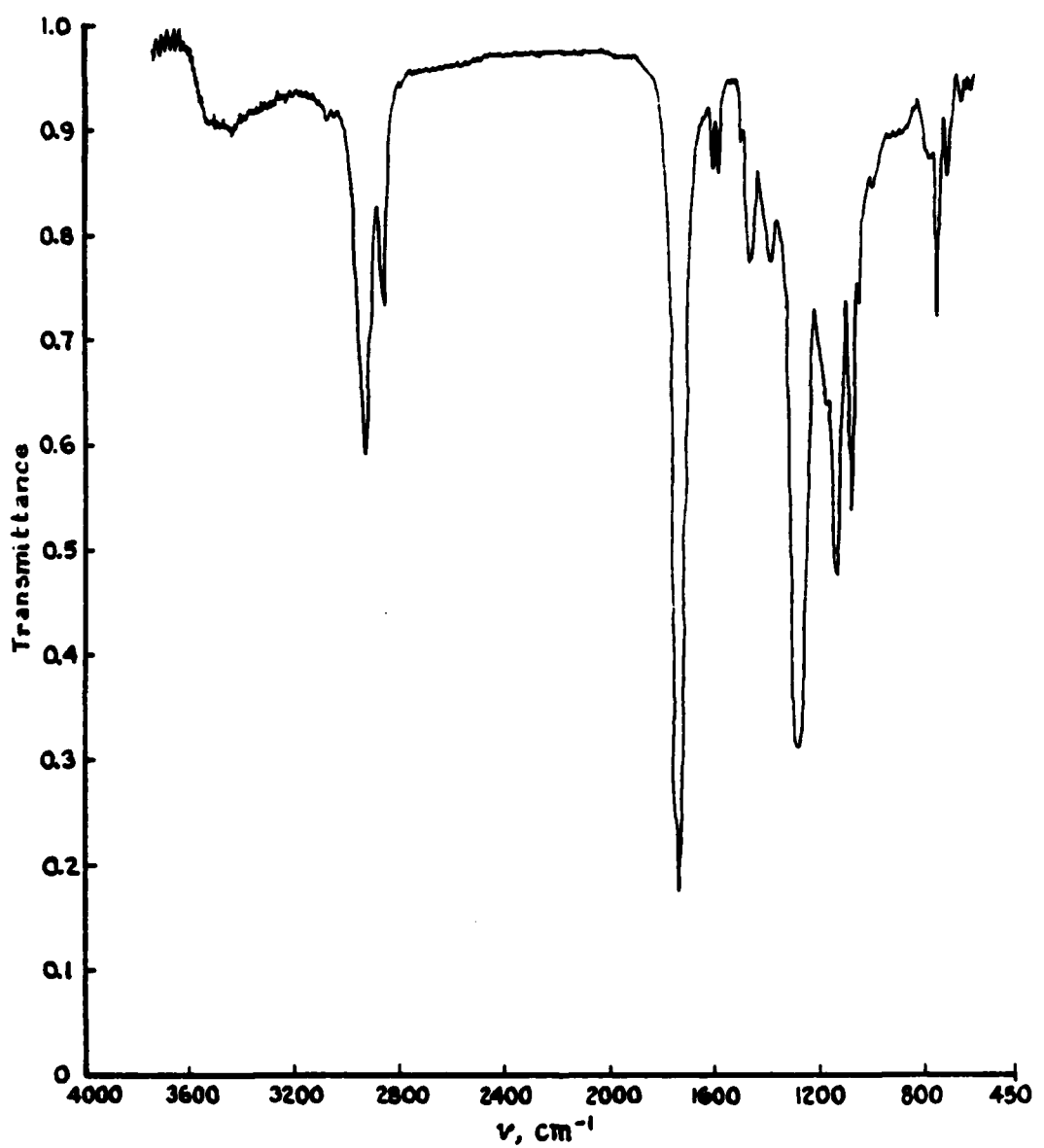
PELLET SPECTRUM OF TALC IN KBr

Figure 6



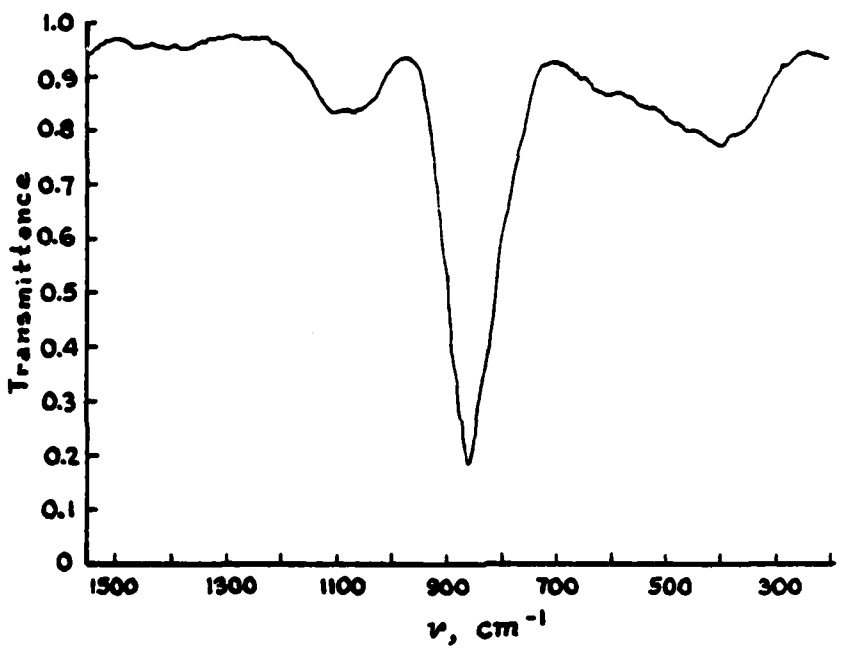
PELLET SPECTRUM OF CARBAZOLE DIOXAZINE VIOLET IN KBr

Figure 7



ALKYD RESIN FILM TRANSMITTANCE AT BREWSTER ANGLE

Figure 8



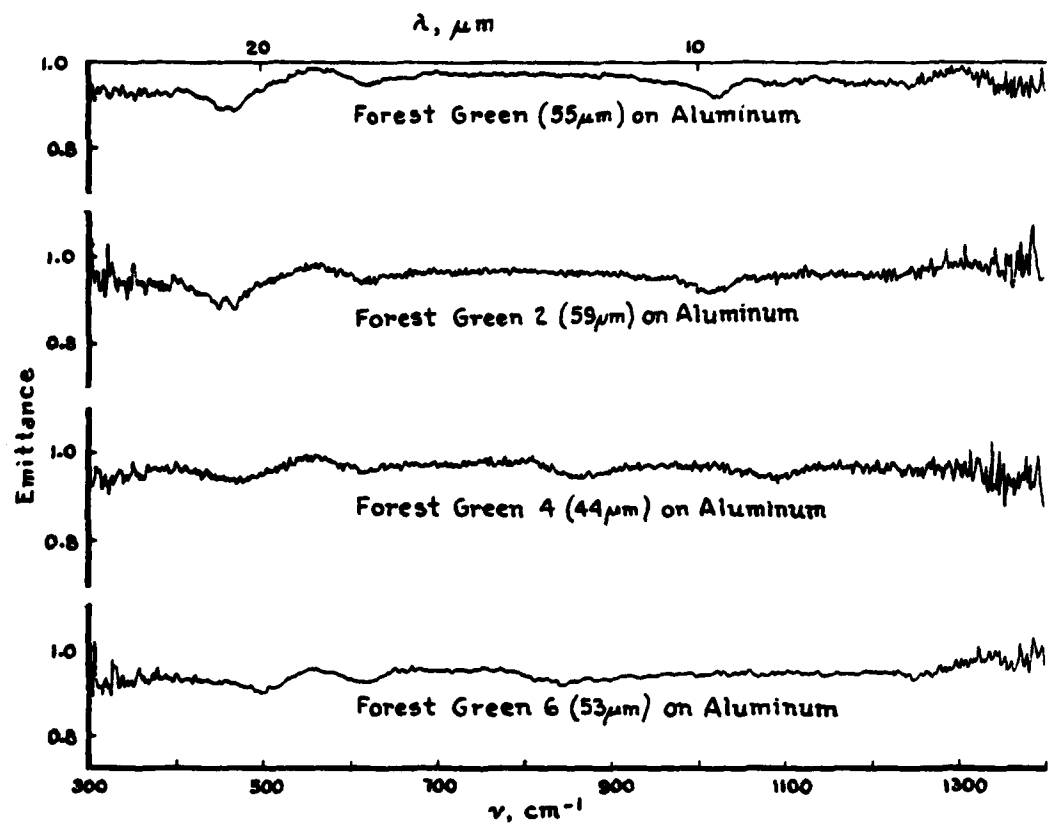
PELLET SPECTRUM OF MOLYBDATE ORANGE

Figure 9

difficult owing to the scattering that occurs at the interfaces between the particles and the medium in which these are dispersed. As will be seen in the next section, the reflection spectra of the acid insoluble green pigment and the crocoite were used to obtain the optical constants of these materials and the transmission spectrum of the alkyd resin was used invoking a new technique (vide infra) to obtain the optical constants of this resin binder.

In order to carry out our modeling calculations in the absence of detailed refractive indices of the other components and also to gain further insight into the properties of the Forest Green formulations, we asked for and were supplied by MERADCOM with a number of subformulations (formulations with various ingredients left out) of the Forest Green paint. These include what we refer to as FG2, FG3, FG4, and FG6, all listed in Table I. The last material was used in this work for a first simulation in the Forest Green system. It should be noted that as FG6 has no extender pigment, it is rather glossy appearing in the visible region. However, it must be noted that in the thermal infrared the distinction between pigments and extender pigments (those which do not contribute color) is completely lost as both the talc and the diatomaceous earth have strong absorption bands and so produce infrared "color."

The thermal emittance spectra of each of these paints except FG3 was obtained by painting a layer on an aluminum plate, and the emittance spectra obtained with our Michelson Interferometer Spectrometer² are shown in Figure 10. Another set of runs on FG4 at a greater layer thickness (74 μm vs 44 μm) showed washed out spectral features with a slightly higher emittance level. We believe the washed out features result simply from the closeness of approach to an emittance of unity caused by the greater layer thickness. Included in our experimental work on the emittance of these materials in the 7-35 μm



EMITTANCE SPECTRA OF FOREST GREEN SYSTEMS

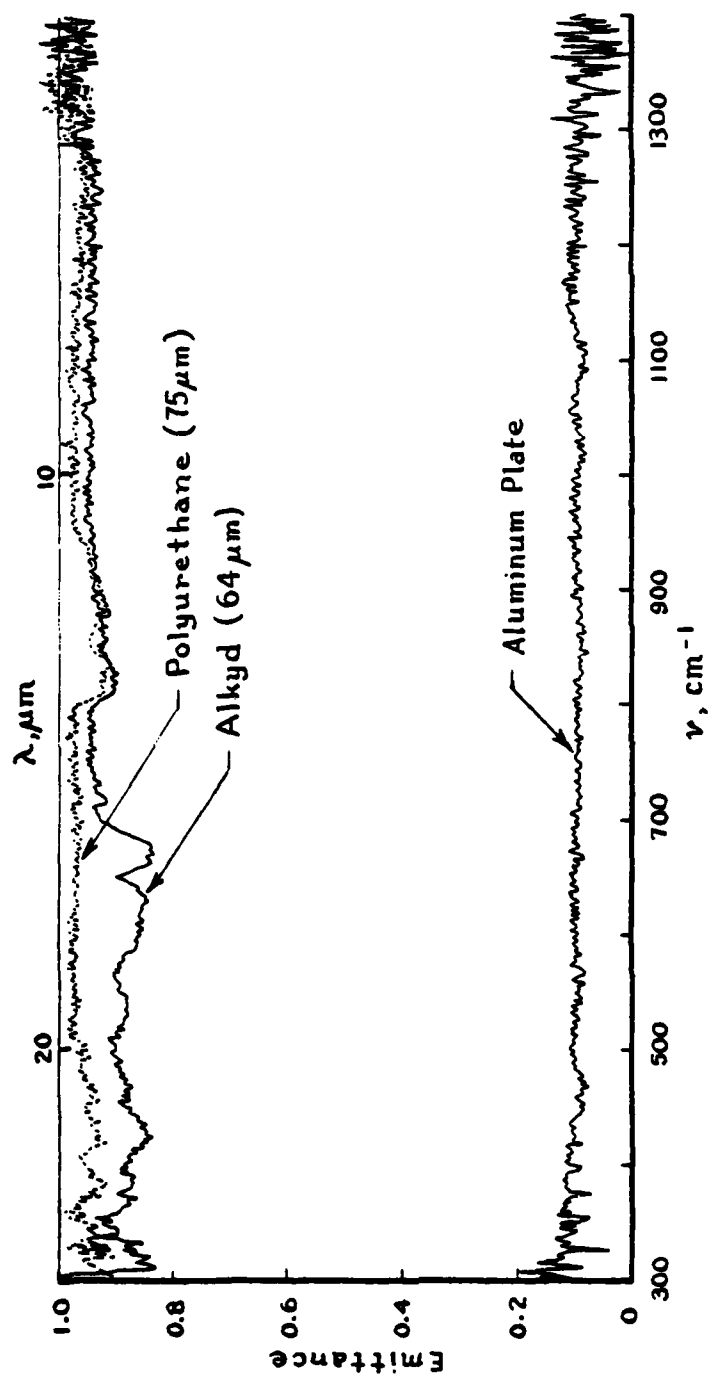
Figure 10

range were measurements made on the underlying substrate aluminum plate and measurements made on the alkyd binder alone and a possible substitute polyurethane binder (Figure 11). All of these spectra were obtained in duplicate runs with the average deviation between the runs being 0.05 (± 0.025). These spectra were obtained using two blackbodies at different temperatures as calibration sources.

The samples of Forest Green paint and subformulations FG4 and FG6 were then run on our Digilab Fourier transform spectrometer in reflectance and the spectra are shown in Figures 12 through 14. These spectra are all necessarily qualitative inasmuch as no reliably known reflectance standard was at hand. Some of these were run against the reflectance of the unpolished substrate material (aluminum) and some against a coarse aluminum scatter plate in our possession. The latter is probably a somewhat better standard as it is a more diffuse reflector having an almost spectrally flat value of 0.2 from about 600 to 4000 cm^{-1} . Clearly a diffuse reflector is a requirement for a standard to be used with diffuse samples as a specular standard does not allow for the energy reflected outside of the acceptance cone of the optical system. The problem then becomes one of relating the angular distribution of the sample and standard properly.

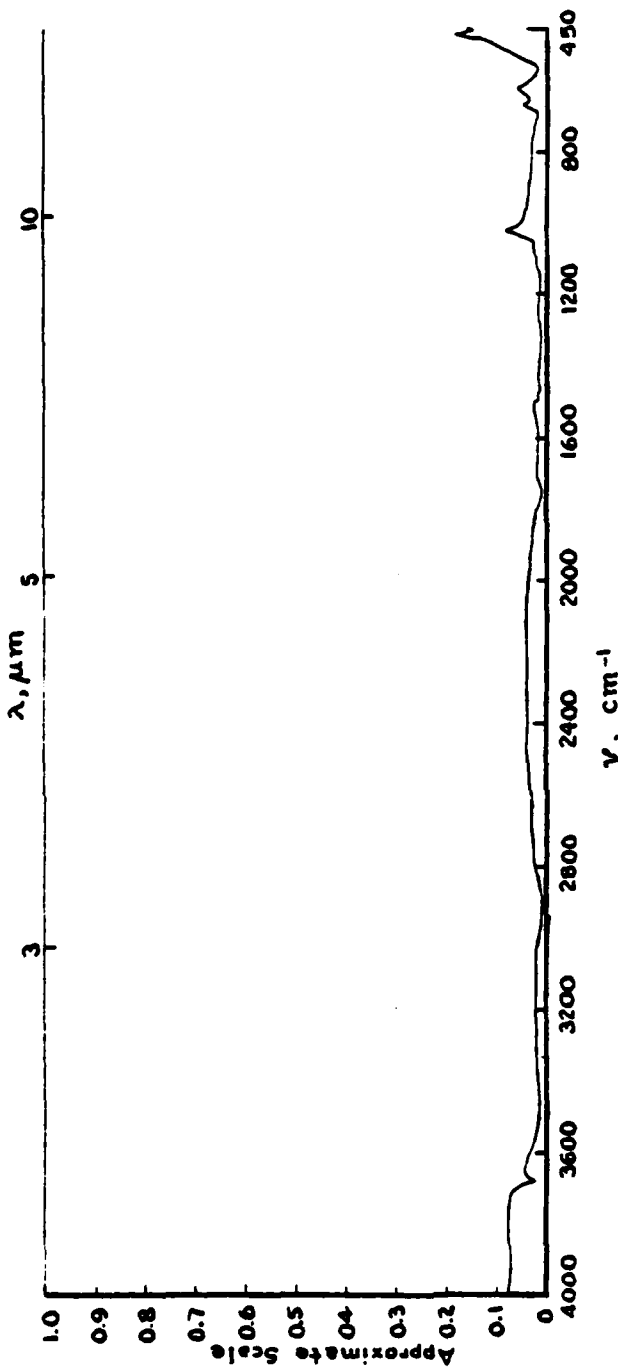
As sufficient work to precisely calibrate our reference plates has not been carried out we consider all spectra measured in reflection in the Digilab instrument to be qualitative in nature and the easiest method of making these quantitative would be to refer them by Kirchhoff's law to our emittance spectra in the $7\text{-}35\text{ }\mu\text{m}$ range. The greater spectral detail observed in reflectance is largely the result of scale expansion and a better signal-to-noise ratio.

Comparisons of various spectra indicate that the qualitative appearance of the various bands follows Kirchhoff's law well (e.g., Figure 15), and that the data are quite accurate



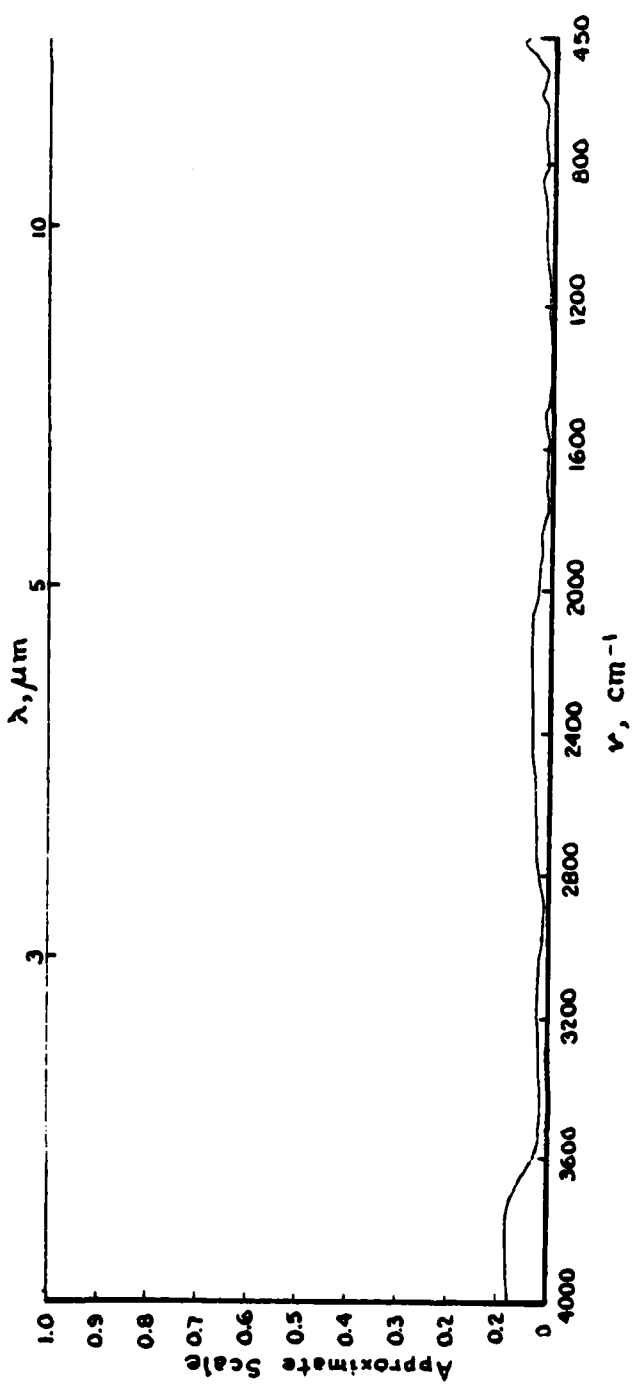
AUXILIARY EMITTANCE DATA

Figure 11



REFLECTANCE OF FOREST GREEN PAINT

Figure 12



REFLECTANCE OF FOREST GREEN 4

Figure 13

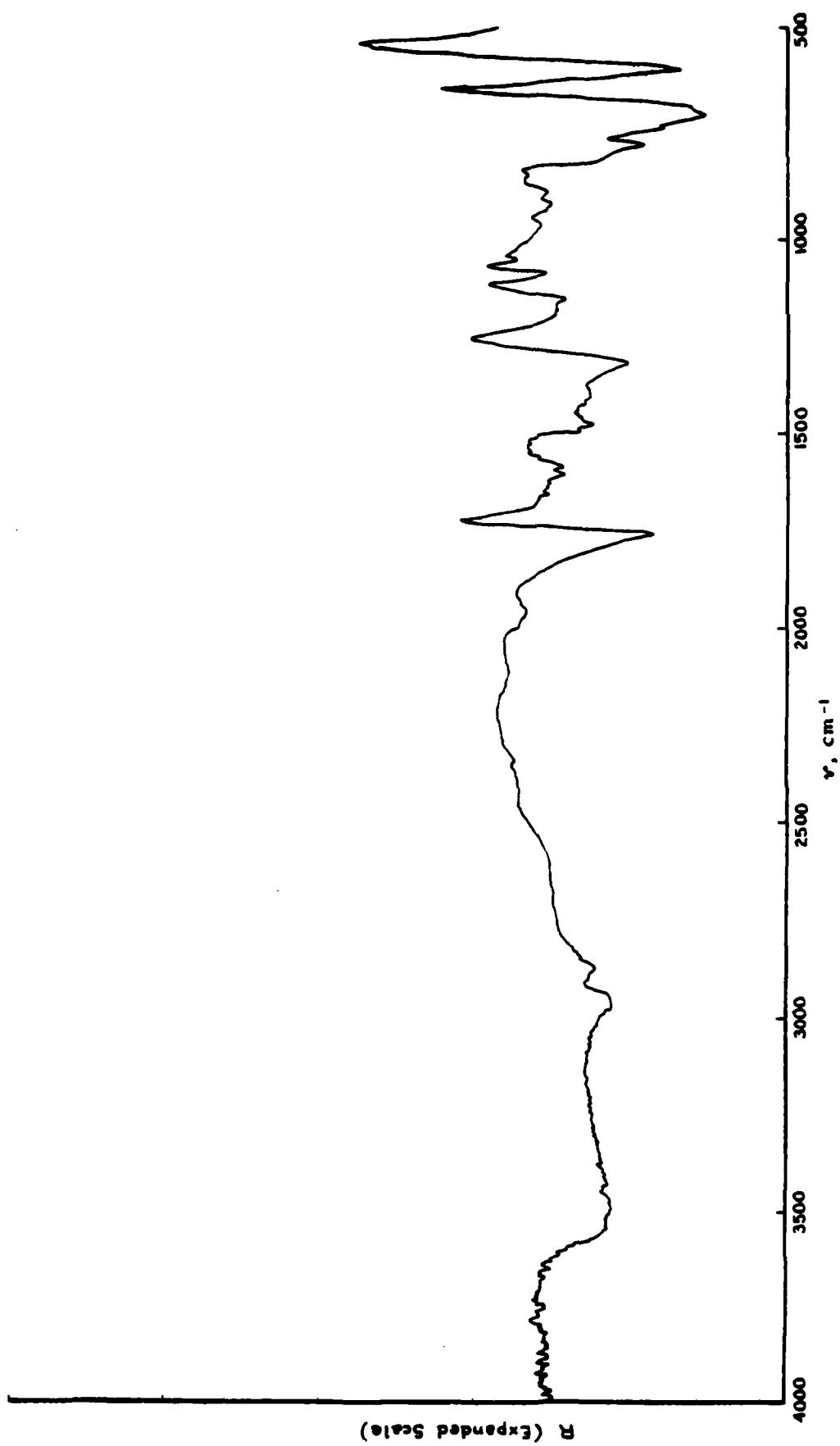
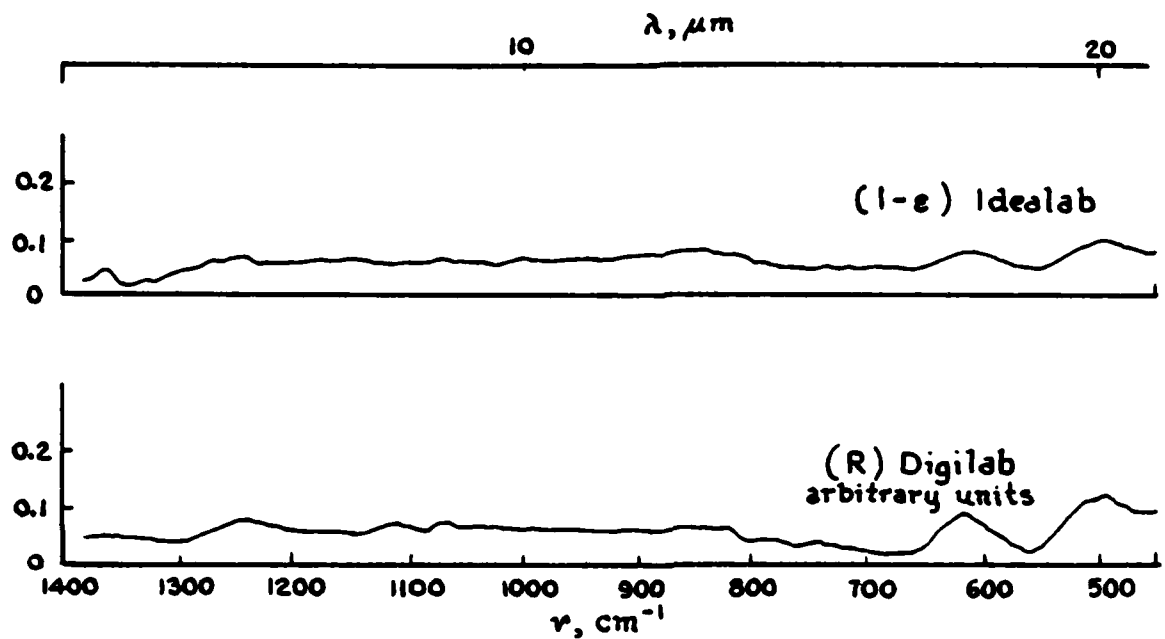


Figure 14



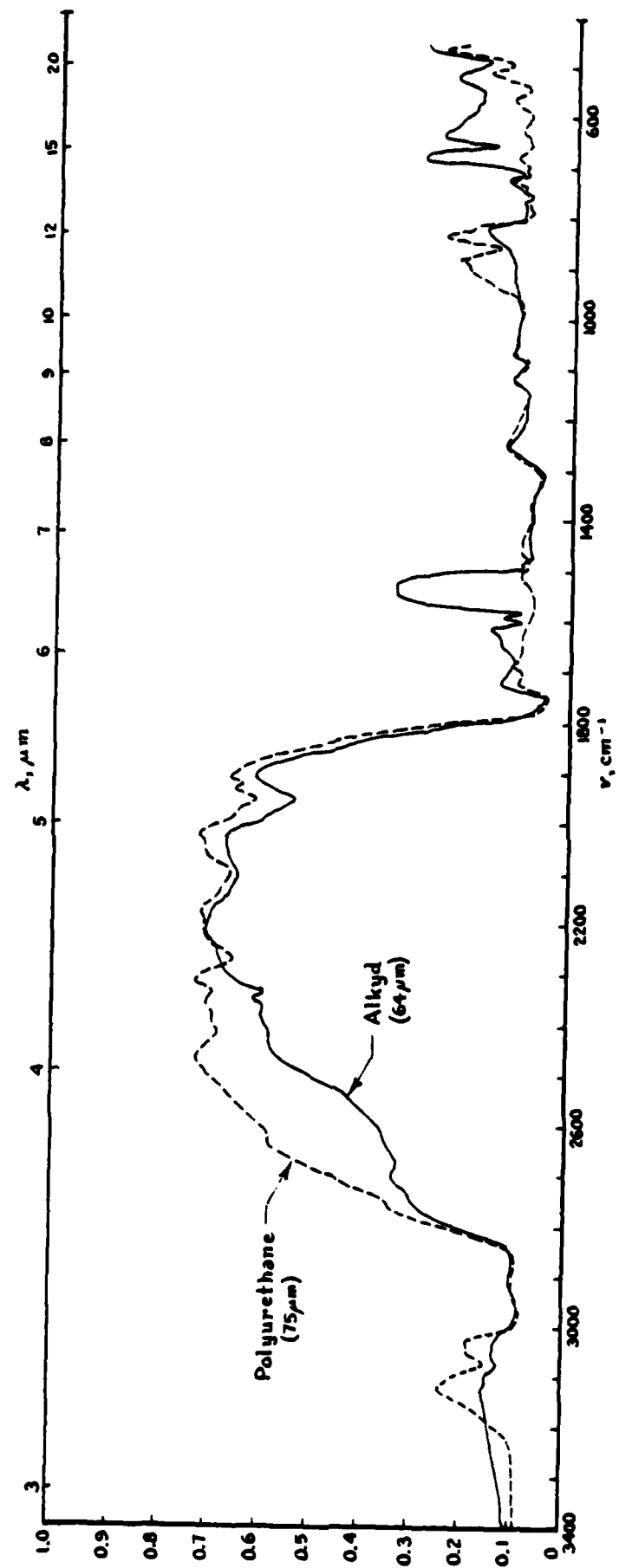
COMPARISON OF EMITTANCE AND REFLECTANCE DATA
FOR FOREST GREEN 6

Figure 15

with respect to spectral shape over the whole range of the measured spectrum.

Reflectance data from the alkyd binder is shown in Figure 16. The low reflectance shown by this film in the 8-14 μm region should be contrasted with the relatively higher value in the 3.5-5.5 μm region. In the same figure, we show a comparable spectrum of the polyurethane binder that has been suggested as a possible replacement for the alkyd binder for contamination resistance¹¹. The data on the polyurethane binder was obtained after it became apparent from our spectra that no combination of pigments could substantially reduce the thermal emittance in the 8-14 μm region below approximately 0.9 inasmuch as the alkyd binder itself had that level of emittance in this region. As can be seen from Figure 16, the polyurethane binder is no better and as a consequence of these results we are led to state that no paint will provide a suitably low emittance in the 8-14 μm region if it is produced using either the alkyd or polyurethane binders.

In fact, it may be very difficult to find an appropriate organic binder if, as we believe, it is necessary to reduce the emittance from values close to unity to values of less than 0.3 over the appropriate thermal band. We have suggested that measurements be made in the future on paraffins to ascertain whether these are feasible substitute binders, in the sense of being capable of providing a suitable physical material for a paint binder and, if that is possible, of providing a sufficiently low binder absorption such that the binder itself will not constitute a primary source of thermal emission. A simple way to view this problem is that by Kirchhoff's law, the emittance is equal to the absorptance so that any substance that absorbs well will emit well. Thus the problem is reduced to one of finding a sufficiently transparent binder that the binder itself does not constitute a



REFLECTANCE OF ALKYD AND POLYURETHANE BINDERS ON ALUMINUM

Figure 16

thermally bright source and thus may be used as a matrix to contain materials which scatter the radiation sufficiently to allow for a low emittance composite material. We will discuss this again further in Section VI.

IV. Optical Constants (Complex Refractive Indices)

In order to carry out our theoretical simulations, we require as input parameters

1. particle size or size distribution
2. volume fractions of the various components, and
3. the spectral complex refractive index of each material.

We were able to obtain such information during this contract by using our previously reported technique¹⁰ for a hot pressed sample of the acid insoluble green pigment (fit shown in Figure 2), and the single crystal crocoite (fit shown in Figure 4) sample. As the molybdate orange and carbazole dioxazine violet are present only in very small quantities, we chose, owing to the present limitations of time and funding to neglect these for our initial comparisons. We attempted to obtain a talc sample with sufficient polish to obtain a good reflection spectrum but some difficulty was obtained in getting a sufficiently specular surface and so that material had to be abandoned for the time being. Qualitative measurements based on the pellet spectra could of course be used to get approximate optical constants for any of these materials, but we chose to try to obtain the best optical constants possible for the first paint simulations. The diatomaceous earth presents an extreme problem in obtaining a homogeneous smooth sample for optical constant determination. For the relatively transparent alkyd binder, a reflection spectrum does not show sufficiently strong bands to be able to use our previous technique of fitting specular reflectance to obtain optical constants. Therefore, we chose

to use a transmission spectrum of a thin film of this material. Some difficulty was encountered in attempting to obtain a sufficiently smooth, homogeneous film of the binder. Reduction of the data from our films by the usual transmission techniques involving the full transmittance equation, including reflection losses, was considered likely to involve some error, owing to the lack of optical perfection of the film surfaces.

In order to circumvent this difficulty, we have chosen to use a somewhat different technique based on measurements of the transmission of the best quality film that we could obtain, at the Brewster angle. The Brewster angle, ϕ is defined by $n = \tan \phi$, where n is the real part of the complex refractive index of the medium. At the angle of incidence ϕ , radiation whose electric vector is in the plane of incidence cannot be reflected, so for this particular angle, and with the use of a polarizer that passes only such radiation, the reflection loss will be zero. That being true, the usual law for thick samples (without interference phenomena)

$$T = \frac{(1-R)^2 e^{-\alpha x}}{1-R^2 e^{-2\alpha x}}$$

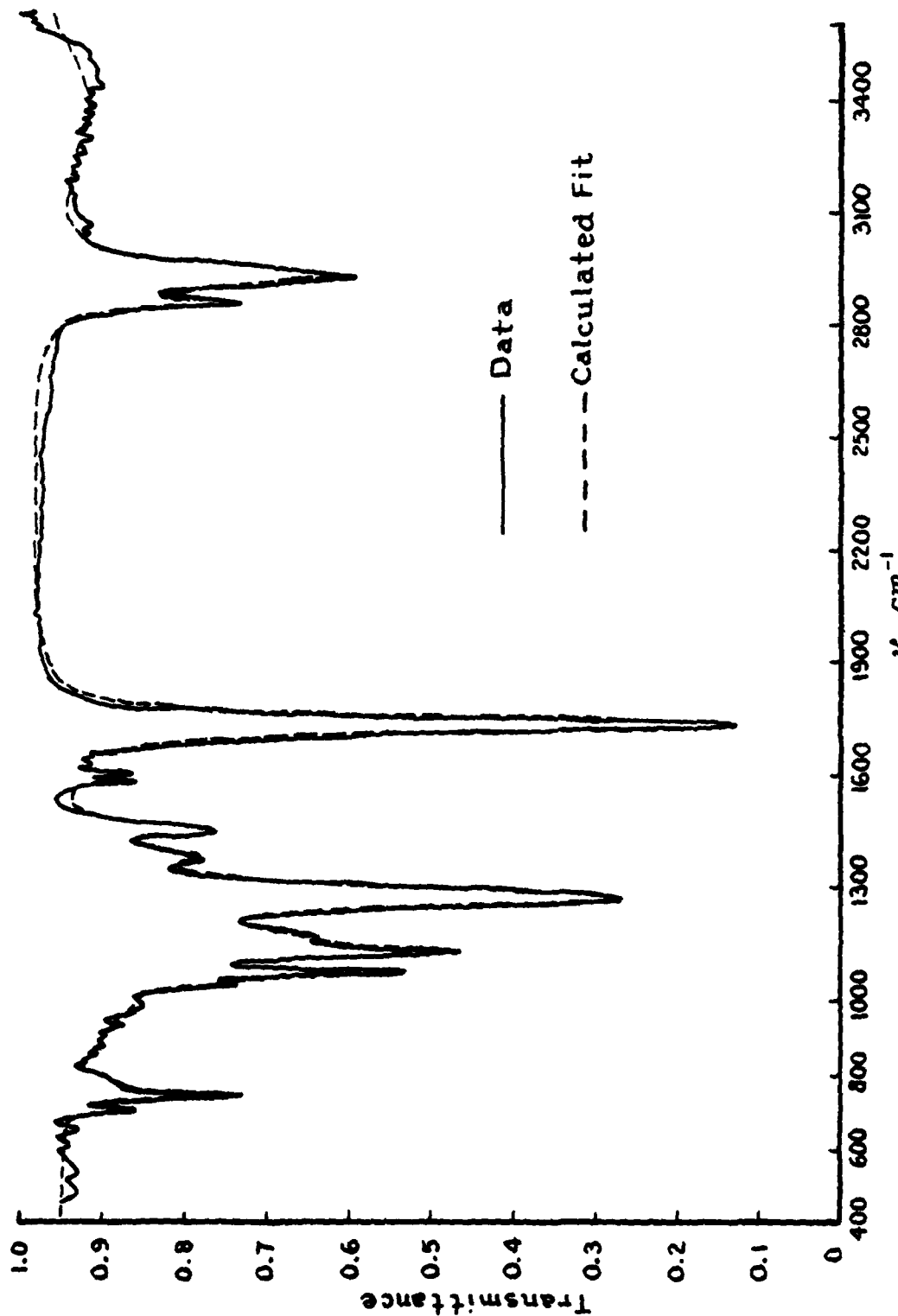
is simplified to $T = e^{-\alpha x}$. Thus we were able to avoid problems involving a least squares fit to the reflection losses where the reflectance is from an imperfect surface. Of course no polarizer is perfect and spectral variations in the value of n would in principle lead to varying values of Brewster's angle. For organic films, however, the dispersion of the refractive index is quite small and an error analysis indicated that the method should be quite accurate.

The results of our standard technique for fitting reflectance data to a set of Lorentz line parameters (classical dispersion theory oscillators) are shown in Figures 2 and 4 for the acid insoluble green hot pressed sample and the

crocoite sample measured at 30° angle of incidence. The crystal orientation for the latter was 9° from the 100 face. This was the only face we could obtain for this monoclinic crystal in sufficiently large size for our measurements. An attempt to hot press a sample of lead chromate powder in the same way as carried out with the acid insoluble green pigment failed owing to chemical reactivity. Therefore, the Lorentz line parameters found from this arbitrary face of the crocoite sample represent some combination of the three sets of line parameters that should be used to represent this monoclinic material. However, the principal line, which is found to be at 823 cm^{-1} , Table II, is seen to correspond roughly to the observed transmission of the pellet spectrum (Figure 3) which shows one large absorption band centered near 840 cm^{-1} . The figure, however, does indicate some evidence of structure in this band which probably indicates contributions from the other orientations of the material. A lower intensity feature near 400 cm^{-1} did not provide a sufficiently strong band in the reflection spectrum of our orientation of crocoite to utilize a second line in our Lorentz line parameter fit although there is some evidence for its presence (see Figure 4). A fit with more lines could probably be attempted but was not carried out as crocoite was not used in our initial modeling.

The Lorentz line fit to the acid insoluble green sample is shown in Figure 2, and the Lorentz line parameters are given in Table III. The strength of the two lines will clearly dominate the model spectrum in the low frequency region so that the small crocoite line mentioned above is undoubtedly unnecessary.

For the alkyd resin, a thin film having a thickness of $2.6 \mu\text{m}$ was fitted by the Brewster angle technique. The Lorentz line parameters for the alkyd film are given in Table IV, and the fit is shown in Figure 17. As can readily be seen, the strengths of these lines are much less than those of the acid



FIT TO ALKYD RESIN TRANSMITTANCE

Figure 17

insoluble green and the crocoite samples. This is the reason that insufficiently strong reflectance spectra could be obtained, but the transmission technique can be seen to have worked quite well. As will be shown later, in the thicknesses of paint layers commonly used, these lines are sufficiently strong to produce features and to emit strongly.

Table II

Crocoite

Estimated standard deviations are given in parentheses

$$\epsilon_{\infty} = 6.2066 \quad (0.0646)$$

v	s	γ
823.32 (1.53)	1.68338 (0.03449)	0.05146 (0.00183)

Table III

Acid Insoluble Green Pigment

Estimated standard deviations are given in parentheses

$$\epsilon_{\infty} = 4.5228 \quad (0.0800)$$

v_j	s_j	γ_j
491.93 (1.04)	3.60492 (0.06646)	0.03733 (0.00219)
611.37 (0.79)	0.66597 (0.02100)	0.03409 (0.00163)

Table IV

Alkyd Film

Estimated standard deviations are given in parentheses

$$\epsilon_{\infty} = 2.3716$$

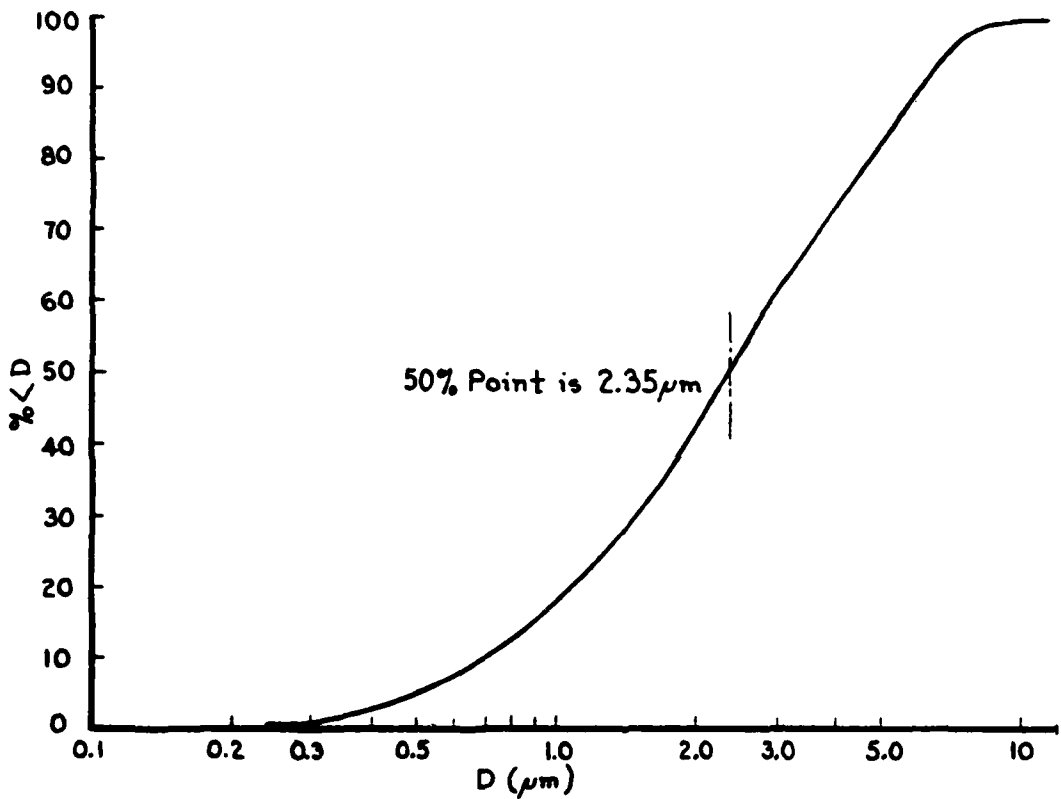
J	v_j	s_j	γ_j
1	3360.35	(7.23)	1.693E-03 (7.872E-05)
2	2932.26	(0.64)	1.807E-03 (4.305E-05)
3	2856.83	(0.66)	3.043E-04 (2.309E-05)
4	1730.94	(0.19)	9.787E-03 (1.149E-04)
5	1599.37	(1.21)	1.928E-04 (4.654E-05)
6	1580.26	(0.91)	1.612E-04 (4.033E-05)
7	1456.20	(0.89)	1.500E-03 (1.037E-04)
8	1387.16	(1.45)	1.408E-03 (1.456E-04)
9	1273.28	(0.33)	2.058E-02 (2.996E-04)
10	1175.07	(1.64)	3.514E-03 (5.132E-04)
11	1128.39	(0.57)	1.007E-02 (5.885E-04)
12	1071.62	(0.40)	4.151E-03 (2.816E-04)
13	1041.27	(1.14)	1.099E-03 (2.974E-04)
14	976.50	(11.97)	9.532E-03 (2.247E-03)
15	469.96	(240.55)	1.326E-01 (1.468E-01)
16	781.88	(5.64)	2.258E-03 (9.357E-04)
17	743.68	(0.52)	3.950E-03 (4.509E-04)
18	704.56	(1.13)	1.046E-03 (2.456E-04)

The Brewster angle technique which we have used in this program is, we believe, novel and will adequately produce Lorentz line parameter fits for relatively weakly absorbing materials in the same manner that the stronger materials can be fitted by reflection techniques. We, therefore, believe that we have techniques for almost any kind of sample if a homogeneous film or plate can be prepared.

V. Comparison of Theoretical Simulations with Experimental Measurements

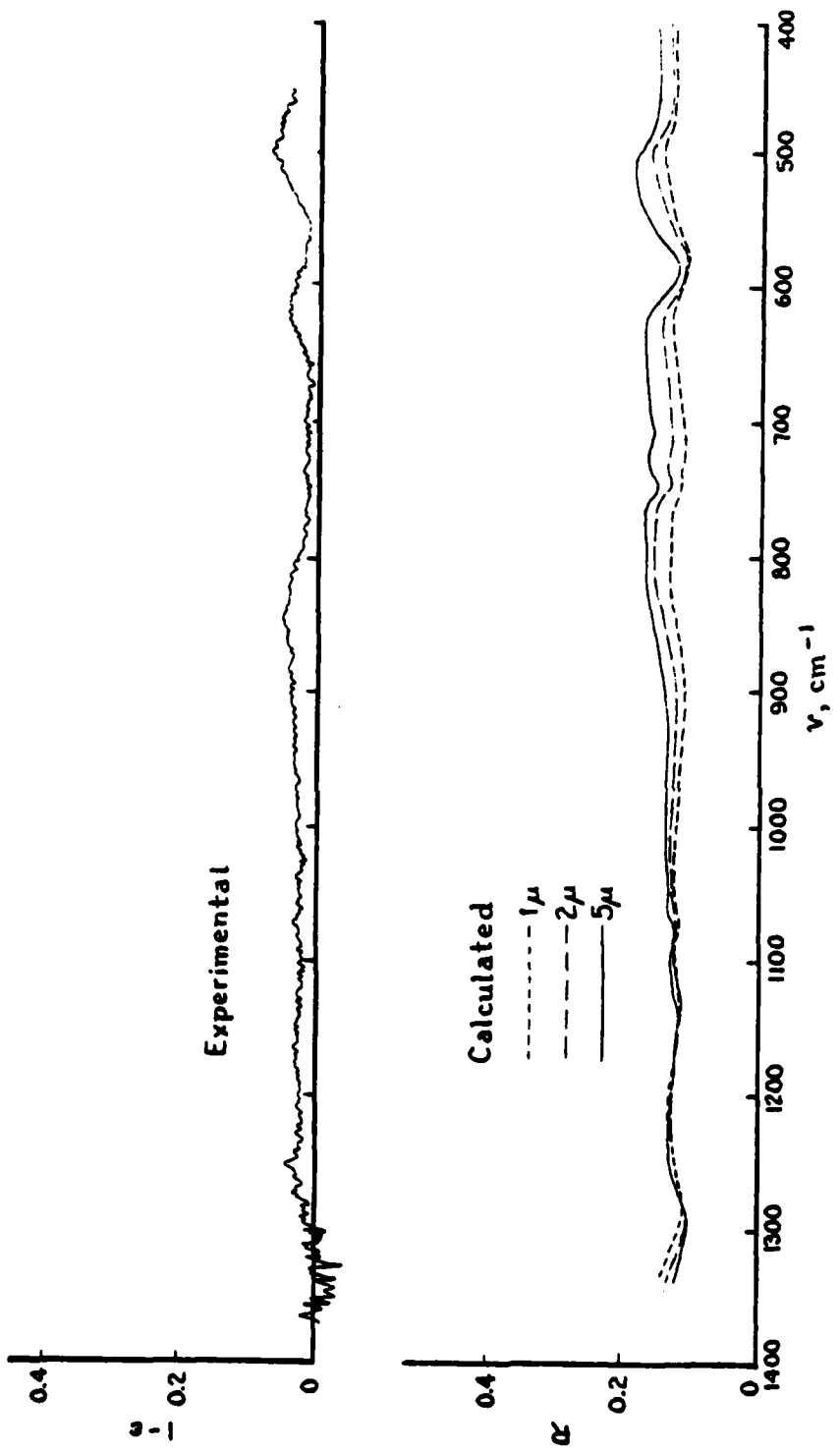
As a test case of the ability of our model to predict the spectral signature of the Forest Green paint system, we have chosen the FG6 paint, which consists only of the alkyd binder and the acid insoluble green pigment for modeling purposes. Figure 18 shows the particle size distribution of the acid insoluble green pigment supplied to us by Mr. Aladar Burgyan of the Ferro Corporation. With this curve as a guide, we selected monodisperse particle diameters of 1, 2, and 5 μm for the purpose of modeling the variations with particle size that may be expected in the range of the particle sizes present. The results of our first simulations are shown in Figure 19 for these three particle sizes. These may be compared with the emittance measurements on the FG6 formulation made by our Michelson interferometer and the qualitative reflectance measurements made on our Digilab system shown in Figure 15.

The emittance data are redrawn in Figure 19 to facilitate the detailed comparison. The important point to note is the approximate match in overall spectral level and the generally accurate major features near 500 and 630 cm^{-1} resulting from the AIG pigment. The discrepancy in spectral level observed ($\Delta R = \Delta \epsilon \sim 0.1$ or 10% in emittance) is partially due to the use of $R_g = 0.9$ (From Figure 11) rather than the value for the over-coated substrate. It also is likely to involve some of our experimental error, as all the emittance spectra shown in this report were from typical single runs rather than averaged with the duplicate runs. That some of the detailed small discrepancies observed are probably the result of small inaccuracies in our bridging relationships is shown in Figure 20 where the



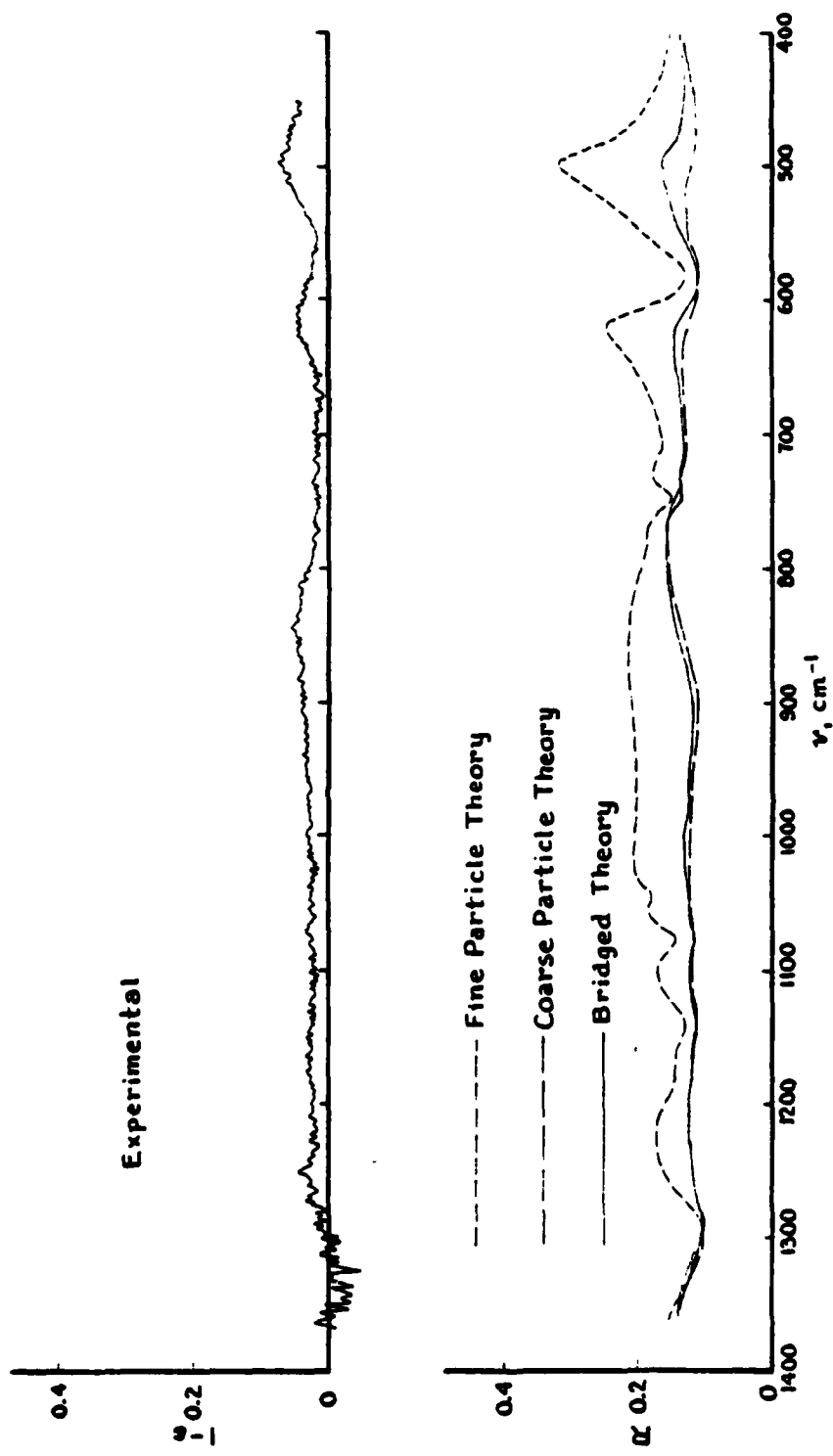
PIGMENT PARTICLE SIZE DISTRIBUTION

Figure 18



COMPARISON OF THEORETICAL SIMULATIONS OF
FOREST GREEN 6 PAINT WITH EXPERIMENTAL DATA
(EFFECT OF PIGMENT PARTICLE SIZE)

Figure 19



COMPARISON OF COARSE, FINE, AND BRIDGED THEORY
SIMULATIONS WITH EXPERIMENTAL DATA

Figure 20

separate contributions of the coarse and fine particle theories are shown together with the combined result. It can be seen that the fine particle theory produces the best qualitative fit to the location and relative importance of the various spectral features but the poorest level when compared to the emittance data. A somewhat modified bridging rule would be expected to improve the overall situation.

VI. Suggestions for Further Work

As discussed above, we consider the basic problem of reducing the thermal emittance of any paint to be principally one of finding a relatively transparent binder in the thermal infrared region. As existing binders tend to be quite opaque even in very thin layers, we have discussed with Mr. Buccigross of our staff, the possibility of finding a new binder that might satisfy the transmission requirement. He posed for us a number of possible materials, and after having surveyed his list and also the infrared characteristics expected for such films, we have come to the conclusion that the best organic type binder would necessarily be one involving some type of paraffin, polyethylene, or rubber material. These materials are not presently available in a form suitable for making a paint, and so in order to develop such a paint or a coating some development work along the lines of producing such a vehicle would be required. Inorganic binders should also be considered.

Assuming an effective bland binder could be developed, it is expected that the visible and near infrared properties would be quite similar to those presently obtained with the existing camouflage paints by using the same pigments especially if the binder refractive index is near 1.5. In the thermal infrared, however, the pigments would have to be modified as the present ones are far from ideal. This requirement would have to be satisfied without substantially degrading the performance of the paints in the visible and near infrared regions.

Further modeling work along the lines begun in this report should be carried out using the candidate binders and improved pigments required for the improved paint formulations in order to optimize particle sizes and volume fractions.

VII. References

1. A.G. Emslie and J.R. Aronson, Appl. Opt., 12, 2563 (1973).
2. J.R. Aronson and A.G. Emslie, Appl. Opt., 12, 2573 (1973).
3. J.R. Aronson and A.G. Emslie, "Applications of Infrared Spectroscopy and Radiative Transfer to Earth Sciences," in Infrared and Raman Spectroscopy of Lunar and Terrestrial Minerals, C. Karr, Jr. Ed., Academic Press, New York, N.Y., 1975.
4. G. Mie, Ann. Phys., 25, 377 (1908).
5. P. Kubelka and F. Munk, Z. Tech. Phys., 12, 593 (1931).
6. J.R. Aronson, A.G. Emslie, E.M. Smith and P.F. Strong, Proc. Lunar Planet. Sci. Conf. 10th, 1787 (1979).
7. J.R. Aronson, A.G. Emslie, F.E. Ruccia, C.R. Smallman, E.M. Smith and P.F. Strong, Appl. Opt., 18, 2622 (1979).
8. D.B. Judd, J. Opt. Soc. Am., 57, 445 (1967).
9. L.C. Afremow and J.T. Vandeberg, J. Paint Tech., 38, 169 (1966).
10. J.R. Aronson and P.F. Strong, Appl. Opt., 14, 2914 (1975).
11. "Investigation of Factors Relative to the Adoption of Two-Component Polyurethane Paint for Army Equipment," DARCOM Polyurethane Paint Task Force, Dec. 1978.

Appendix 1

THEORY OF THE SPECTRAL REFLECTANCE OF A LAYER OF PAINT ON A SUBSTRATE

For mathematical convenience we consider that the layer of paint consists of one or more kinds of pigment particles embedded in a continuous binder which extends for a small distance in front of the pigment particles and also behind them. The thin film of pure binder at the front gives a well-defined gloss component of the reflectance. The thin film of binder at the back is assumed to be in good optical contact with the substrate and therefore provides a definite value of the back reflectance R_g . We also assume, again for mathematical tractability, that the light is everywhere completely diffuse.

The radiative transfer in the paint layer can be described in terms of the well-known two-flux model of Kubelka and Munk⁽⁵⁾. This theory yields the general solution:

$$I = Ae^{-\gamma x} + Be^{\gamma x} \quad (A1)$$

$$J = R_V Ae^{-\gamma x} + \frac{1}{R_V} Be^{\gamma x} \quad (A2)$$

where I and J are respectively the ingoing and outgoing diffuse fluxes at a distance x from the front surface of the paint layer.

A and B are arbitrary constants which are determined by the boundary conditions at the front and back of the layer.

R_v is the volume reflectance of the pigment-binder medium, i.e., the ratio J/I of the outgoing to ingoing flux that would exist if the paint layer extended to infinity.

The quantity γ is the extinction coefficient of radiation in an infinite medium, and includes the effect of both scattering and absorption losses in the medium.

R_v and γ are related to the diffuse absorption and scattering coefficients K and S by the relations:

$$R_v = 1 + \frac{K}{S} - \left[\left(\frac{K}{S} \right)^2 + 2 \left(\frac{K}{S} \right) \right]^{1/2} \quad (A3)$$

$$\gamma = K^2 + 2KS \quad (A4)$$

For given values of the complex index of refraction $m = n - ik$ of the pigment particles and the binder, and the average particle size and packing density, we can calculate K and S by means of a theory ^(1,3) developed by us for powders. We have to modify this theory for the case of particles immersed in a binder by replacing the complex index m of the particles by the relative index m/n_0 of a particle with respect to the binder, and at the same time use the radiation wavelength λ/n_0 in the binder in place of the free-space wavelength λ .

The boundary conditions needed to determine the constants A and B in Equations (A1) and (A2) will now be considered. At the back interface, located at $x = X$, the boundary condition is simply:

$$J(X) = R_g I(X) \quad (A5)$$

At the front surface the boundary conditions are somewhat more complicated. The incident diffuse radiation strikes the binder surface and is partially reflected. We calculate the corresponding external diffuse reflectance R_e by integrating the Fresnel reflectance over all angles of incidence. The fraction of the radiation entering the binder is therefore $1-R_e$.

Back-scattered diffuse radiation arriving at the binder surface internally is also partially reflected. The internal diffuse reflectance R_i is not equal to R_e . If a piece of dielectric material of index n_o is imagined to be put in a cavity at some temperature T the radiation flux in the dielectric, under thermodynamic equilibrium conditions, is n_o^2 times as large as in the empty part of the cavity. This implies that, for equilibrium to be maintained, the external and internal transmission coefficients T_e and T_i through the surface of the dielectric must satisfy the condition:

$$T_e = n_o^2 T_i \quad (A6)$$

It follows that:

$$R_i = 1 - \frac{1-R_e}{n_o^2} \quad (A7)$$

In terms of R_e and R_i the boundary conditions at the front surface, $x = 0$, are:

$$I(0) = (1-R_e)I_o + R_i J(0) \quad (A8)$$

$$J_o = R_e I_o + (1-R_i)J(0) \quad (A9)$$

where I_o and J_o are the incident and reflected diffuse fluxes.

The diffuse reflectance R is given by:

$$R = \frac{J_o}{I_o} \quad (A10)$$

On applying the above boundary conditions to Equations (A1) and (A2) we find, after some algebra, that:

$$R = \frac{\left[R_e (1 - R_i R_v) (1 - R_v R_g) - R_e (R_v - R_i) (R_v - R_g) e^{-2\gamma x} \right.}{\left. + (1 - R_e) (1 - R_i) R_v (1 - R_v R_g) - (1 - R_e) (1 - R_i) (R_v - R_g) e^{-2\gamma x} \right]}{(1 - R_i R_v) (1 - R_v R_g) - (R_v - R_i) (R_v - R_g) e^{-2\gamma x}} \quad (A11)$$